

Two-photon geometrical phase

D. V. Strekalov and Y. H. Shih

Physic Department, University of Maryland Baltimore County, Baltimore, Maryland 21228

(Received 7 February 1997)

An advanced wave model is applied to a two-photon interference experiment to show that the observed interference effect is due to the geometrical phase of a two-photon state produced in spontaneous parametric down-conversion. The polarization state of the signal-idler pair is changed adiabatically so that the ‘‘loop’’ on the Poincaré sphere is opened in the signal channel and closed in the idler channel. Therefore, we observed an essentially nonlocal geometrical phase, shared by the entangled photon pair, or a biphoton.

[S1050-2947(97)03509-9]

PACS number(s): 42.50.Dv, 03.65.Bz

The term *geometrical phase*, or *Berry phase*, refers to the phase gained by a particle during a cyclic adiabatical evolution [1]. Numerically, this phase is equal to the solid angle confined by the evolution trajectory on the Poincaré sphere, multiplied by the spin of the particle.

In optics, the geometrical phase is also known as the Pancharatnam phase [2]. The optical geometrical phase has been studied actively by several researchers; see, e.g., [3]. A typical interferometer that can be used to observe the Pancharatnam phase is described in [4]. It splits a light beam in two parts: one undergoes cyclic polarization evolution and the other is used as a reference. As the beams are mixed by the output beam splitter, interference fringes arise that depend on the geometrical phase as well as on the dynamical phase.

Feeding a similar interferometer with the *signal* beam from a spontaneous parametric down-converting crystal [5] and using the *idler* beam to trigger a coincidence circuit, an experimental study of the geometrical phase in a single-photon regime has been carried out [6]. Alternatively, the same type of interferometer can be fed with two-photon light emitted in a *collinear* down-conversion process [7]. Then again *either* the signal *or* the idler undergoes the cyclic polarization evolution, allowing the single-photon geometrical phase to be measured.

In this paper we wish to report an experiment with a geometrical phase shared by an entangled photon pair. We ‘‘open’’ the ‘‘loop’’ on the Poincaré sphere in the idler channel and ‘‘close’’ it in the signal channel. Then the cyclic polarization evolution is experienced not by a single photon but by the *biphoton*. To explain the above statement, let us point out that the fully consistent description of two-photon phenomena is given by a two-photon wave packet (biphoton) rather than in terms of two single-photon wave packets (although in some cases these notations lead to the same result) [8].

Equivalent to the biphoton notation, but perhaps a more pictorial description is given by the *advanced wave* model [9]. The advanced wave model takes advantage of reversibility of the Green’s function describing propagation of light wave from a space-time point (\vec{r}, t) to a space-time point (\vec{r}', t') :

$$G(\vec{r}, t; \vec{r}', t') = -G^*(\vec{r}', t'; \vec{r}, t).$$

This allows us to replace the ‘‘conventional’’ propagating idler [10] wave by an advanced wave, propagating from the detector towards the source backward in time. In the framework of this model, one detector can be considered as a light source and the pump wave fronts in the crystal as geometrical reflecting mirrors [11]. A pure two-photon geometrical phase will be observed if the cyclic polarization evolution begins in the idler channel before the ‘‘turning point’’ (the crystal) and is completed after it in the signal channel, without altering dynamical phases.

The experimental setup is shown in Fig. 1. A cw ultraviolet pump with wavelength $\lambda_p = 351$ nm from an argon-ion laser is converted by a 3-mm-long β -barium-borate (BBO) crystal into the signal and idler radiation with the same (degenerate) central wavelength $\lambda = 702$ nm. The BBO is cut for type-II phase matching, which means that one component of the emitted radiation is polarized vertically (along the y axis) and the other one is polarized horizontally (along the x axis). A detailed analysis of the type-II down-conversion can be found in [12]. The crystal orientation is chosen so that both vertical and horizontal components can be emitted into both the signal and the idler modes. Therefore, the polarization part of the two-photon state is entangled [12]:

$$|\Psi_0\rangle = (|x\rangle_1 |y\rangle_2 + |y\rangle_1 |x\rangle_2) / \sqrt{2}. \quad (1)$$

Due to birefringency of the BBO, the ordinary (x -polarized) wave is delayed with respect to the extraordinary (y -polarized) wave. To compensate for this effect an

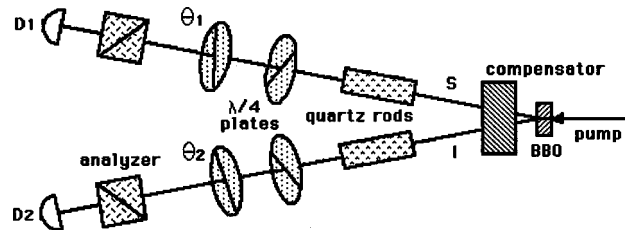


FIG. 1. Scheme of the experiment. The signal (S) and idler (I) from a down-converting crystal BBO pass through the compensator and the quartz rods. The polarization of the signal and idler is manipulated by two pairs of $\lambda/4$ wave plates, then projected onto linear polarization states by two analyzers, and sent to detectors D_1 and D_2 for coincidence detection.

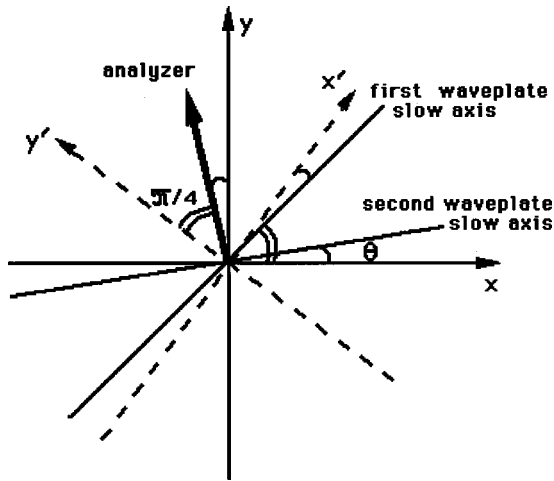


FIG. 2. Orientations of the quarter wave plates and the analyzer in the signal channel. The x' and y' are polarization directions of the x and y components after they pass two quarter wave plates. In the idler channel, the orientation of the first quarter wave plate is 90° off, which leads to swapping the axes x' and y' .

other birefringent crystal is used whose relative optical delay is equal to *one-half* of the BBO delay [12]. In our experiment it is a 14-mm quartz crystal. After the compensator, there is a 4-cm crystal quartz rod in each channel. In the signal channel the rod's axis is horizontal and in the idler channel the rod's axis is vertical. The rods introduce approximately $360\text{-}\mu\text{m}$ delay between the x and y polarization components, which exceeds the signal and idler coherence length determined by the interference filters (placed in front of the detectors D_1 and D_2) to be $160\text{ }\mu\text{m}$. This once again emphasizes that we deal with two-photon effects and no single-photon effects are relevant.

The polarization state of the signal and idler is manipulated by two zeroth-order quarter wave plates and a polarization analyzer likewise in both channels. The orientations of those elements in the signal channel are shown in Fig. 2. In the idler channel the orientations of all elements are the same, except for the first quarter wave plate, which is 90° off with respect to Fig. 2. The angle θ is a "free" parameter in each channel. It determines the geometrical phase ϕ gained in each channel.

The first quarter wave plate in the signal channel transforms the linear polarization along the x axis to left-hand circular polarization and the linear polarization along the y axis to right-hand circular polarization (vice versa in the idler channel). The second quarter wave plate transforms the circular polarization back to a linear one along the x' and y' axes (see Fig. 2). The polarization states $|x'\rangle$ and $|y'\rangle$ are orthogonal because they are obtained from the orthogonal polarization states $|x\rangle$ and $|y\rangle$ by a unitary transformation.

The fact that quarter wave plates transform circular polarization to linear has been used for making circular polarization analyzers. In those devices a linear analyzer makes 45° with the quarter wave plate axis. Thus if, for example, the right-hand polarization is transformed by the quarter wave plate to a linear polarization that passes the analyzer, then the left-hand polarization is completely blocked. This is *not* what happens in our setup. As shown in Fig. 2, the analyzer is set at 45° with respect to the (x', y') basis, so that

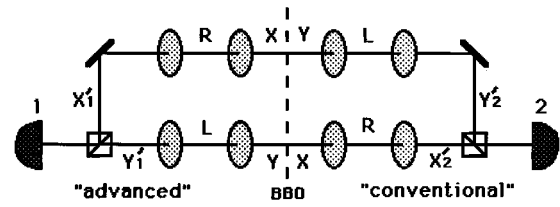


FIG. 3. Scheme equivalent to the one in Fig. 1 in advanced wave notation.

equal fractions of the x' - and y' -polarized (and hence of the x - and y -polarized) light pass the analyzer. This has to be constantly maintained as the angle θ varies, which is achieved by rotating the analyzer together with the quarter wave plate and hence together with the (x', y') basis.

Let us now describe our experiment in terms of the advanced wave model (Fig. 3). The detector D_1 is assigned to be a source. Its "radiation" is split by a polarizer to the x'_1 and y'_1 components. These components propagate through the same path, but in Fig. 3 they are shown to go by different paths for convenience. In the course of its propagation, the x'_1 component is transformed by the quarter wave plates first to $|R\rangle$ and then to $|x\rangle$ polarization states [13]. When the state $|x\rangle$ reaches the "turning point" marked by a vertical dashed line, it suddenly (nonadiabatically) turns to the $|y\rangle$ state, which propagates conventionally (forward in time) through the next two quarter wave plates. Its polarization state subsequently becomes $|L\rangle$ and $|y'_2\rangle$.

Similarly to the upper path in Fig. 3, the polarization state in the lower path undergoes a series of transformations

$$|y'_1\rangle \rightarrow |L\rangle \rightarrow |y\rangle \rightarrow |x\rangle \rightarrow |R\rangle \rightarrow |x'_2\rangle.$$

If $\theta_1 = \theta_2 \equiv \theta$ is maintained in the experiment, the directions x'_1 and y'_2 are the same and so are x'_2 and y'_1 (see Fig. 2 and the caption). Then the polarization state evolution in both upper and lower arms of the interferometer in Fig. 3 is cyclic and the phase measured by this interferometer is equal to the difference of the two-photon geometrical phases. The subtle point is that we have a nonadiabatic jump in the course of the evolution. This is the jump from a linear polarization state to the orthogonal state. We will assume now and prove later (in the Appendix) that the resulting phase does not affect the observable interference pattern and thus may be ignored.

The evolution of the phase state in the upper and lower paths in Fig. 3 is represented in the left and right parts of Fig. 4, respectively. The Poincaré spheres are drawn according to the tradition [14]. It is easy to see that the geometrical phase gained in the upper path is determined by the angle θ to be

$$\phi_1 = \frac{1}{2} [\pi + 2\theta - (\pi - 2\theta)] = 2\theta.$$

Likewise the phase in the lower part $\phi_2 = -2\theta$ and we may expect interference fringes of the shape $1 - \cos 4\theta = \sin^2(2\theta)$ (the minus sign is due to reflections) to appear in coincidences.

To experimentally test the above prediction, we turned the rotatable quarter wave plates in the signal and idler channels of our setup starting from the x direction with the same step

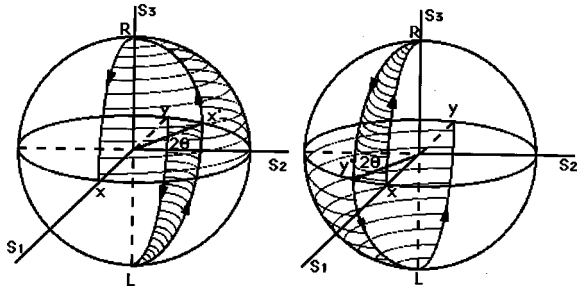


FIG. 4. Evolution of the polarization state in the upper (left) and lower (right) paths in Fig. 3 mapped onto the Poincaré sphere. On the left sphere, we start from x' on the equator and move to x via the north pole (R). The covered solid angle is $\pi + 2\theta$. Then we jump to y and return to x' via the south pole (L). The covered solid angle is $-(\pi - 2\theta)$. Similarly, on the right sphere, we start from y' on the equator and move via the south pole to y , then jump to x , and return to y' via the north pole.

10° at a time. At the same time the analyzers were rotated with the same step and in the same direction as the plates, but starting from the y direction (see Fig. 2). Thus four optical elements were rotated simultaneously.

The experimental result shown in Fig. 5 agrees with our prediction, clearly demonstrating the effect of the two-photon geometrical phase. The solid line is a \sin^2 fitting curve and the circles are the data points. Squares are also data points obtained in the case when the quarter wave plates and analyzers in the signal and idler channels were rotated in *opposite* directions, $\theta_1 = -\theta_2 \equiv \theta$. In this case the coincidence counting rate is on the level of noise and no fringes were observable. We will discuss this result later. As was expected, the single counting rates of the detectors remained constant (Fig. 6).

The result $R_c \propto \sin^2(2\theta)$ can also be obtained without using the advanced wave model, by standart quantum-mechanical calculations. We performed such calculations in the Appendix. Its result indicates that the interference effect can also be observed when $\theta_1 \neq \theta_2$, that is, the geometrical phase arises even if the contour on the Poincaré sphere is not closed. This generalization agrees with the definition of relative phase ϕ between two arbitrary states $|\psi\rangle$ and $|\psi'\rangle$ [15,16]:

$$\phi = \arg(\langle \psi | \psi' \rangle).$$

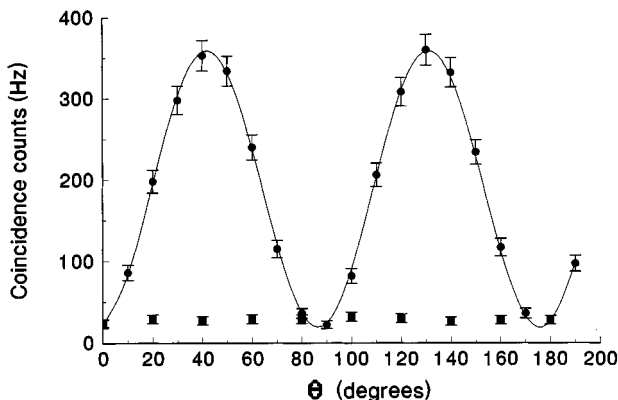


FIG. 5. Coincidence counting rate vs the angle θ . Circles are data points for $\theta_1 = \theta_2 \equiv \theta$, squares are data points for $\theta_1 = -\theta_2 \equiv \theta$, and the solid line is a sine square fit.

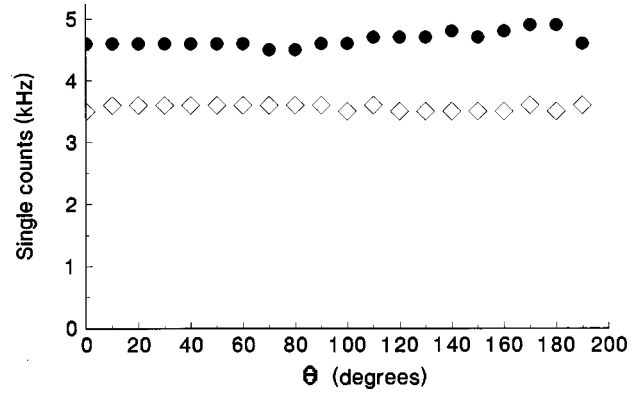


FIG. 6. Single counting rates vs the angle θ .

Moreover, a straightforward analysis shows that the same type of interference fringe is observed if the second quarter wave plates are removed altogether from both channels. Such experiments were actually performed in connection with Bell's theorem testing, using circular polarization, entangled states [17]. Now we see that the two-photon interference effects exploited in those experiments for violation of Bell's inequalities can be understood as a manifestation of the two-photon geometrical phase. The connection of such a phase with the Bell's inequalities is that the same issue of nonlocality is approached from two different directions.

However, it is not easy to find a "classical" analog to the experiments [17] like we did for our experiment using the advanced wave model (Fig 3). One needs an optical device that splits a linear polarization in circular polarizations and sends the right-hand polarization to one channel and the left-hand polarization to the other. Of course, the simplest realization of such a device is a usual linear polarizer with a quarter wave plate in each of its output channels, but then we get back to our present setup shown in Fig. 1.

It is important to emphasize that we measured a pure biphoton geometrical phase with no contribution of dynamical phase. The dynamical phase of a single particle may be defined as [15,18]

$$\phi_d = \frac{1}{\hbar} \int_{t_i}^{t_f} E(t) dt. \quad (2)$$

For a spontaneous parametric down-conversion photon pair the individual photon energies are uncertain, but the total energy is exactly equal to $\hbar \omega_p$ [5]. Therefore, we can write Eq. (2) in the form

$$\phi_d = \int_{\text{path}} \frac{\omega_p}{u} dl,$$

where u is the group velocity. Notice that the path length does not change during the experiment, nor does the group velocity for a circularly polarized wave as it passes through a rotated quarter wave plate. Therefore, the relative dynamical phase remains constant and does not add to the observed interference effect.

To conclude, we have observed a two-photon geometrical phase that is due to an adiabatic change of the polarization state of an entangled two-photon system, a biphoton. The advanced wave interpretation of this effect is analogous to

the ‘‘classical’’ optical geometrical phase; however, our effect is observable in the fourth-order correlation of the fields (in coincidence counts). Therefore, we have studied one more aspect of the ‘‘two-photon optics,’’ which belongs with the two-photon geometrical optics [11] and two-photon wave optics [19] effects. The fundamental object in this optics is the biphoton that is considered an essentially nonlocal physical entity, not less ‘‘realistic’’ and not more mysterious than a photon in the traditional optics.

This work was supported by Office of Naval Research Grant No. N00014-91-J-1430.

APPENDIX

Let us introduce the x - and y -polarized states in the form

$$|x\rangle \equiv \begin{bmatrix} 1 \\ 0 \end{bmatrix}, \quad |y\rangle \equiv \begin{bmatrix} 0 \\ 1 \end{bmatrix}. \quad (\text{A1})$$

Then the matrix of the polarization transformation due to a quarter wave plate set at angle θ is given by

$$T(\theta) = R^{-1}(\theta)DR(\theta), \quad (\text{A2})$$

where $R(\theta)$ is a rotation matrix

$$R(\theta) = \begin{bmatrix} \cos\theta & \sin\theta \\ -\sin\theta & \cos\theta \end{bmatrix}$$

and D is a quarter period delay

$$D = \begin{bmatrix} i & 0 \\ 0 & 1 \end{bmatrix}.$$

The initial state $|\Psi_0\rangle$ [see Eq. (1)] will be transformed into the state

$$|\Psi\rangle = T_1(\pi/4)T_1(\theta_1)T_2(-\pi/4)T_2(\theta_2)|\Psi_0\rangle, \quad (\text{A3})$$

where the subscripts 1 and 2 refer to the signal and idler channels, respectively.

Substituting Eqs. (A2) and (1) into Eq. (A3) and performing a straightforward but lengthy calculation, we arrive at the final state

$$|\Psi\rangle = ie^{i(\theta_1 + \theta_2 + \pi/2)}|x'_1\rangle|y'_2\rangle + ie^{-i(\theta_1 + \theta_2 + \pi/2)}|y'_1\rangle|x'_2\rangle, \quad (\text{A4})$$

where

$$|x'_1\rangle = \begin{bmatrix} \cos(\theta_1 + \pi/4) \\ \sin(\theta_1 + \pi/4) \end{bmatrix}, \quad |y'_1\rangle = \begin{bmatrix} -\sin(\theta_1 + \pi/4) \\ \cos(\theta_1 + \pi/4) \end{bmatrix}, \\ |x'_2\rangle = \begin{bmatrix} -\sin(\theta_2 + \pi/4) \\ \cos(\theta_2 + \pi/4) \end{bmatrix}, \quad |y'_2\rangle = \begin{bmatrix} \cos(\theta_2 + \pi/4) \\ \sin(\theta_2 + \pi/4) \end{bmatrix} \quad (\text{A5})$$

are linearly polarized states. It is clear from Eq. (A5) that $x'_1 \perp y'_1$, $x'_2 \perp y'_2$, and the analyzers can always be set at 45° with respect to the (x', y') basis. The analyzers make the terms of Eq. (A4) indistinguishable and enable interference. The coincidence counting rate is proportional to

$$R_c \propto |e^{i(\theta_1 + \theta_2 + \pi/2)} + e^{-i(\theta_1 + \theta_2 + \pi/2)}|^2 \propto \sin^2(\theta_1 + \theta_2), \quad (\text{A6})$$

which agrees with the results in Fig. 5 for $\theta_1 = \theta_2$ and $\theta_1 = -\theta_2$. While in the former case the geometrical phases ϕ_1 and ϕ_2 are opposite and the interference fringes have doubled frequency, in the latter case they are equal and no fringes observed. The result (A6) also shows that the non-adiabatic jump that has been discussed earlier does not yield an observable phase contribution.

-
- [1] M. V. Berry, Proc. R. Soc. London, Ser. A **392**, 45 (1984).
[2] S. Pancharatnam, *Collected Works of S. Pancharatnam* (Oxford University Press, London, 1975).
[3] R. Y. Chiao and Y. S. Wu, Phys. Rev. Lett. **57**, 933 (1986); A. Tomita and R. Y. Chiao, *ibid.* **57**, 937 (1986); R. Y. Chiao, A. Antaramian, K. M. Ganga, H. Jiao, S. R. Wilkinson, and H. Nathel, *ibid.* **60**, 1214 (1988).
[4] R. Bhandari and J. Samuel, Phys. Rev. Lett. **60**, 1211 (1988).
[5] The parametric down-conversion process is closely studied in, e.g., W. H. Louisell, A. Yariv, and A. E. Siegmann, Phys. Rev. **124**, 1646 (1961); D. N. Klyshko, *Photons and Nonlinear Optics* (Gordon and Breach Science, New York, 1988); T. G. Giallontenzi and C. L. Tang, Phys. Rev. **166**, 225 (1968).
[6] See, e.g., P. G. Kwiat and R. Y. Chiao, Phys. Rev. Lett. **66**, 588 (1991); T. P. Grayson, J. R. Torgerson, and G. A. Barbosa, Phys. Rev. A **49**, 626 (1994).
[7] J. Brendel, W. Dultz, and W. Martienssen, Phys. Rev. A **52**, 2551 (1995).
[8] In the following paper it is shown that the ‘‘two photons’’ and the ‘‘two-photon’’ approaches are *not* equivalent: T. B. Pittman, D. V. Strekalov, A. Migdall, M. H. Rubin, A. V. Sergienko, and Y. H. Shih, Phys. Rev. Lett. **77**, 1917 (1996).
[9] J. G. Cramer, Phys. Rev. D **22**, 362 (1980); D. N. Klyshko, Sov. Phys. Usp. **31**, 1 (1988).
[10] Of course it is rather arbitrary which wave is to be advanced, the signal or the idler, as much as assigning the names ‘‘signal’’ and ‘‘idler’’ to the down-conversion beams.
[11] T. B. Pittman, Y. H. Shih, D. V. Strekalov, and A. V. Sergienko, Phys. Rev. A **52**, R3429 (1995); T. B. Pittman, D. V. Strekalov, D. N. Klyshko, M. H. Rubin, A. V. Sergienko, and Y. H. Shih, *ibid.* **53**, 2804 (1996).
[12] M. H. Rubin, D. N. Klyshko, Y. H. Shih, and A. V. Sergienko, Phys. Rev. A **50**, 5122 (1994).
[13] Notice that the actual wave propagating towards D_1 in the upper path in Fig. 3 passes through the $|L\rangle$ polarization state. This difference is because of the propagation direction reversal. Alternatively, we could preserve the $|L\rangle$ polarization state for the advanced wave, but to assign the opposite sign to the area circled by the advanced wave state on the Poincaré sphere. The same concerns the lower path in Fig. 3.
[14] Max Born and Emil Wolf, *Principles of Optics: Electromag-*

- netic Theory of Propagation, Interference, and Diffraction of Light* (Pergamon, Oxford, 1975).
- [15] Y. Aharonov and J. Anandan, *Phys. Rev. Lett.* **58**, 1593 (1987).
- [16] T. F. Jordan, *Phys. Rev. A* **38**, 1590 (1988); J. Samuel and R. Bhandari, *Phys. Rev. Lett.* **60**, 2339 (1988); R. Bhandari, *Phys. Lett. A* **135**, 240 (1989); D. N. Klyshko, *ibid.* **140**, 19 (1989).
- [17] Y. H. Shih and C. O. Alley, *Phys. Rev. Lett.* **61**, 2921 (1988); Y. H. Shih, A. V. Sergienko, M. H. Rubin, T. E. Kiess, and C. O. Alley, *Phys. Rev. A* **50**, 23 (1994).
- [18] Barry R. Holstein, *Am. J. Phys.* **57**, 1079 (1989).
- [19] P. H. S. Ribeiro, S. Pádua, J. C. Machado da Silva, and G. A. Barbosa, *Phys. Rev. A* **49**, 4176 (1994); **51**, 1631 (1995); D. V. Strekalov, A. V. Sergienko, D. N. Klyshko, and Y. H. Shih, *Phys. Rev. Lett.* **74**, 3600 (1995); Z. Y. Ou, L. J. Wang, X. Y. Zou, and L. Mandel, *Phys. Rev. A* **41**, 566 (1990).